SLAC-PUB-5953
October 1992
E

SLD LIQUID ARGON CALORIMETER

ERIC VELLA
representing the SLD Collaboration

Stanford Linear Accelerator Center
Stanford University
Stanford, CA 94309

ABSTRACT

The liquid argon calorimeter (LAC) of the SLD detector is a parallel plate - liquid argon sampling calorimeter, used to measure particle energies in Z^0 decays at the Stanford Linear Collider. The LAC module design is based on a unique projective tower structure, in which lead plates and segmented lead tiles serve both as absorbers and electrodes. The LAC front end electronics incorporates several novel features, including extensive multiplexing and optical fiber readout, which take advantage of the low SLC beam crossing frequency. The operational performance of the LAC during the recently completed SLD physics run (which recorded over 10000 Z^0 events) is discussed.

Presented at the III International Conference
on Calorimetry in High Energy Physics,
Corpus Christi, Texas, September 29 – October 2, 1992

This work was supported by the U.S. Department of Energy, under contracts DE-AC03-76SF00515

1. Introduction

The liquid argon calorimeter (LAC) of the SLD detector is composed of a cylindrical barrel calorimeter and two endcap calorimeters, forming three distinct mechanical and cryogenic systems, as illustrated in figure 1. The barrel LAC is 6 meters long and extends in radius from 1.8 to 2.9 meters. It is located within the SLD solenoidal magnet and supported by slings from the main arches of the detector. The two endcaps fit just inside the barrel cylinder and are mounted on retractable end doors of the detector. The entire LAC weighs 750 tons. Full details of the LAC design and construction can be found elsewhere.[1]

The LAC cryogenic systems are fairly complex, but operate very smoothly in practice. Inner and outer argon cylinders enclose the calorimeter modules in a common liquid argon volume of 35000 liters. Inner and outer vacuum cylinders provide an insulating vacuum which reduces the heat load to 1000 Watts. Liquid nitrogen flows through cooling loops, at a rate of 10000 liters/day, to regulate the liquid argon temperature.

The LAC provides electromagnetic and hadronic calorimetry over the full azimuth and $|\cos(\theta)| < 0.98$ (the barrel LAC covers $\theta > 33°$, while the endcaps cover $8° < \theta < 35°$). Calorimetry in the barrel-endcap overlap region is degraded by 5 radiation lengths of dewar and support materials.

The LAC has a total thickness of 2.8 absorption lengths, sufficient to contain 80-90% of the energy of the jets in a hadronic Z^0 decay. Energy leaking out of the LAC is measured in the warm iron calorimeter (WIC), an iron plate sampling calorimeter with gas tube readout.

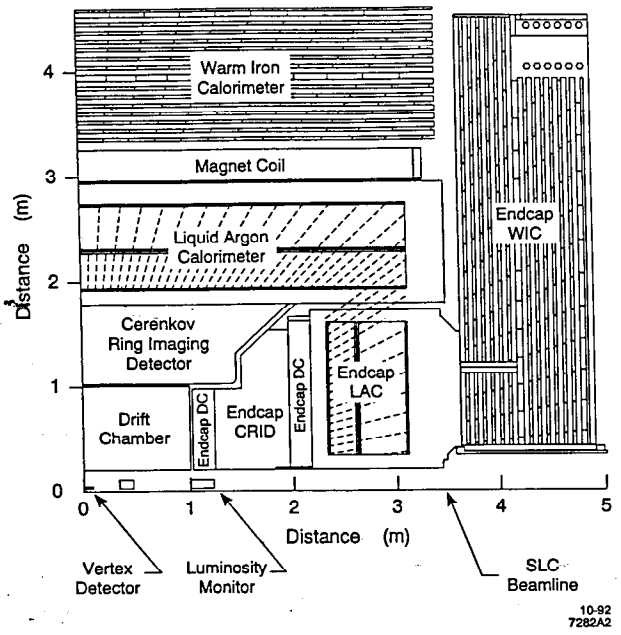

Figure 1. Quadrant view of the SLD detector.

2. Calorimeter Modules

The barrel section of the LAC is composed of 288 modules mounted within the cylindrical cryostat and sharing a common liquid argon volume. The full azimuth of the cylinder is spanned by 48 modules of width $\sim$ 30 cm. The axial (z) direction is spanned by three modules of length $\sim$2 m, attached to and separated by annular "washers" which are integral parts of the cryostat structure. In the radial direction, two separate types of modules – electromagnetic (EM) and hadronic (HAD) – are mounted on top of each other. A drawing of several barrel modules, showing some of the construction details, is shown in figure 2.

The two endcap sections of the LAC are each composed of 16 wedge shaped modules, again mounted within a common cryostat and sharing a common liquid argon volume. Endcap modules incorporate both EM and HAD sections in one mechanical unit. Endcap modules are functionally identical to barrel modules, with similar tower geometry, but there are basic differences in module design and construction. Only barrel modules will be described in detail here.

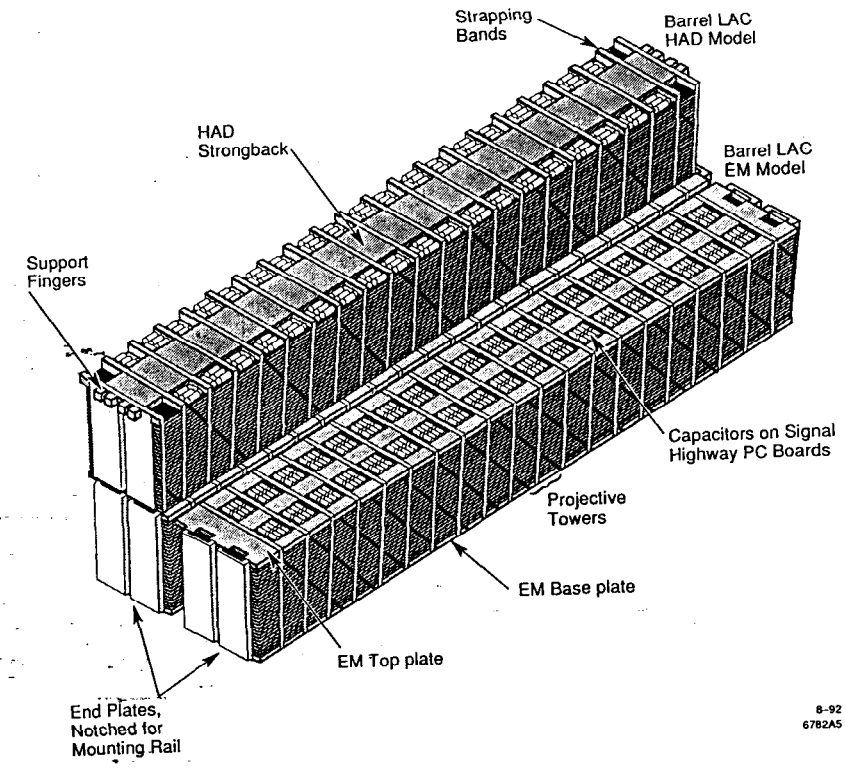

Figure 2. LAC barrel EM and HAD modules.

2.1 Plate and Tile Geometry

LAC modules are constructed as parallel plate liquid argon ionization chambers. The absorber structure consists of alternate planes of large lead sheets and segmented lead tiles, separated and held apart by spacers, with liquid argon filling the gaps between the planes. The tiles in successive planes are arranged transversely and connected radially to form projective towers. The lead plates are grounded, while the tiles are held at high voltage and serve as the charge collecting electrodes. Figure 3 shows a section of a hadronic module stack, illustrating the plate and tile arrangement.

The calorimeter modules are stacked on a thin aluminum support structure, stiffened primarily at the back. The use of lead as both the high Z absorber and the electrode structure makes a compact calorimeter possible. The modules are held together by stainless steel bands wrapped around the open sides, minimizing radial cracks between the modules. The steel bands are wrapped over springs and tensioned to 2g, to hold the modules together by compression in all orientations on the detector.

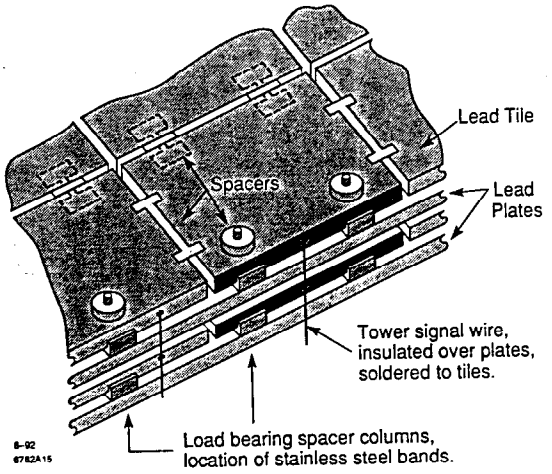

Figure 3. LAC barrel HAD module plate and tile detail.

2.2 Liquid Argon / Lead Sampling

The lead plates and tiles in EM calorimeter modules are 2 mm thick and are separated by 2.75 mm liquid argon gaps. This yields a longitudinal density of 0.79 X_0/cm and a dE/dX sampling fraction (energy deposited in liquid argon / total energy loss, for a minimum ionizing particle) of 18%. The EM calorimetry is divided radially into two separate readout sections to provide information on longitudinal shower development for electron/pion discrimination. The front section (EM1) contains the first 6 radiation lengths of material, while the back section (EM2) contains an additional 15 radiation lengths. The 21 radiation length thickness of the EM calorimetry is sufficient to contain 50 GeV electrons, with leakage (and leakage fluctuations) at the 1-2% level. The energy resolution for electromagnetic showers is expected to be 10-12%, including a 1-2% degradation due to material in front of the calorimeter.

The lead plates and tiles in HAD calorimeter modules are 6 mm thick and are separated by 2.75 mm liquid argon gaps. This yields a longitudinal density of 0.044λ/cm and a dE/dX sampling fraction of 7%. The HAD calorimetry is also divided radially into two separate readout sections (HAD1 and HAD2), each 1 absorption length in thickness. The total EM + HAD thickness of 2.8 absorption lengths is sufficient to contain 80-90% of the energy of a hadron shower; energy leaking out of the LAC is measured in the WIC. The energy resolution for hadrons is expected to be approximately $60\%/\sqrt{(E)}$.

2.3 Tower Segmentation

Transverse segmentation of the LAC is provided by the segmented lead tiles. Tiles from successive layers are laid out in a projective pattern, and stacks of these tiles are ganged longitudinally into towers. The azimuth (ϕ) of the barrel is divided into 192 EM towers, each with an opening angle $\delta\phi = 33$ mrad. The polar angle (θ) of the barrel is divided into 34 EM towers on each side of the midpoint. The tile size increases with polar angle, so as to maintain a constant projective area for electromagnetic showers. The opening angle of an EM tower thus decreases from $\delta\theta = 36$ mrad at the center of the barrel to $\delta\theta = 21$ mrad at the end of the barrel. HAD towers are twice as large as EM towers in both transverse dimensions.

The endcap transverse segmentation continues the general tower arrangement of the barrel. In the EM sections, the azimuthal segmentation is also 192 at large radii, but falls to 96 and then to 48 at the smallest radii, to maintain an approximately constant projective area for electromagnetic showers. The polar angle segmentation follows the same philosophy, with the range $35^0 < \theta < 8^0$ divided into 17 segments. The transverse segmentation in the HAD sections is again twice as coarse as in the EM sections.

2.4 Tower Signal Transmission

Since the calorimeter towers are operated at high voltage, blocking capacitors are needed to couple the signals to the external electronics. The blocking capacitors for each tower have at least four times the tower capacitance, to provide 80-90% charge transfer efficiency. These large capacitors are housed on PC boards mounted on top of the modules, immersed in liquid argon. These PC boards also serve to distribute high voltage to the towers, through individual resistors connected to a common HV bus. Tower signals are routed to the PC boards by tile-to-tile wiring running up along the exposed sides of the module.

A compact cabling scheme connects tower signals to the external electronics, as illustrated in figure 4. Tower signals leave the calorimeter modules on 1-3 meter long ribbon cables which plug into connectors on the PC board. Hermetic feedthroughs in flanges mounted on the argon cryostat endplates carry the tower signals from the argon space to the vacuum space. Feedthroughs on corresponding flanges on the vacuum cryostat endplates carry the tower signals outside the detector. The front-end electronics is mounted directly on these flanges, accessing tower signals directly from the feedthrough signal pins.

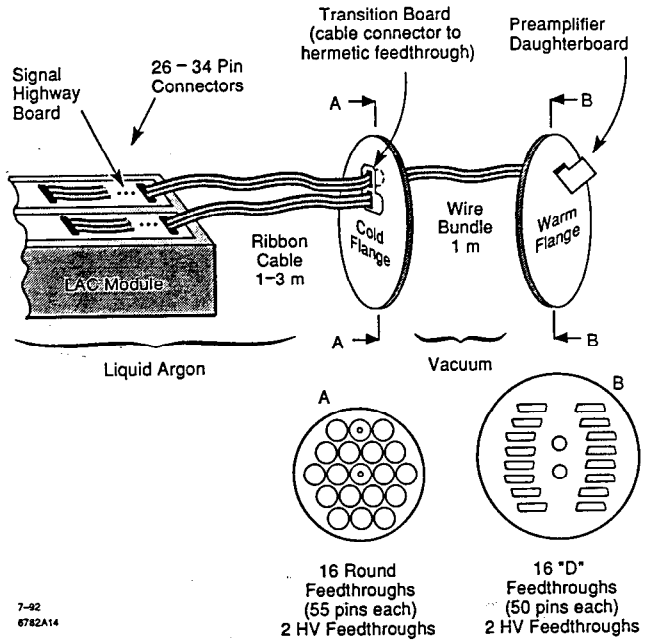

Figure 4. LAC readout cables, flanges, and feedthroughs.

3. LAC Electronics

3.1 Front-end Electronics

The front-end electronics system for the LAC consists of charge sensitive preamplifiers, analog storage and multiplexing devices, analog-to-digital converters, and associated power and control circuits. Performance requirements and detector operating conditions led to a design containing several novel features. These include the installation of the front-end electronics directly on the detector, eliminating completely the need for low level signal cables external to the cryostat, the acheivement of low noise levels without the use of transformers, allowing the electronics to operate inside the detector magnetic field, the extensive use of channel multiplexing to minimize cable plant volume, and the removal of power from the preamplifiers between beam crossings to minimize power dissipation. Extensive use of custom integrated circuits, dense hybrids, and unique packaging makes these solutions practical. The 120 Hz frequency of the SLC beam crossings, allowing over 8 ms between events for online data processing, was exploited throughout the entire electronics chain.

The front-end electronics is packaged in sub-assemblies which, due to their shape, are called "tophats". Tophats are mounted directly on the signal feedthrough flanges on the outside of the liquid argon cryostat. The layout of the electronics within a LAC barrel tophat is shown schematically in figure 5, along with the connections from the detector to the tophat and from the tophat to the external control and data acquisition systems.

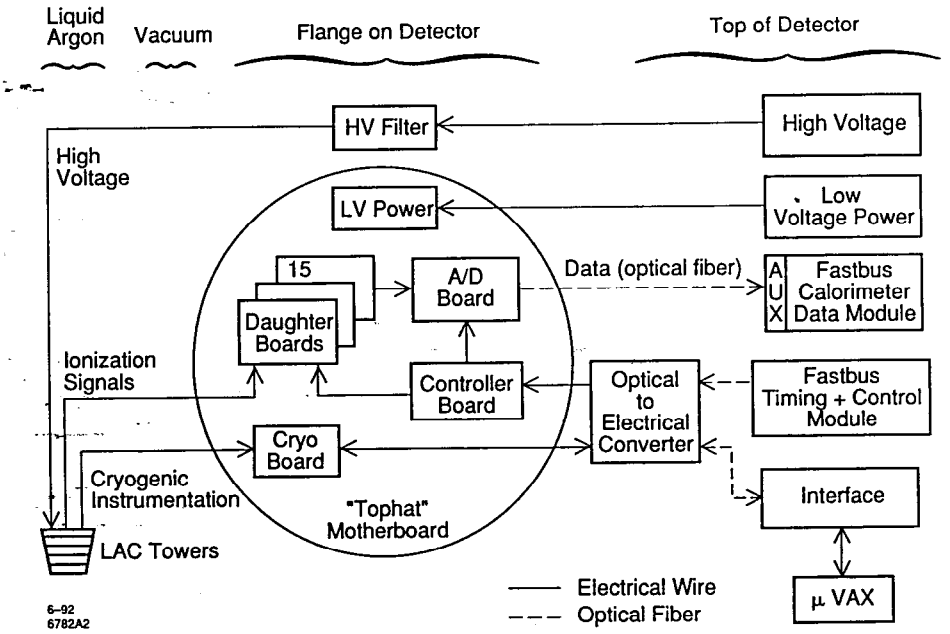

Figure 5. LAC electronics organization.

We have taken advantage of the low SLC repetition rate (120 Hz) to reduce the front-end power consumption by turning off the preamplifiers between beam crossings. Each tophat contains a power supply board which provides local energy storage capacitors and voltage regulation. The preamplifiers are turned on 1 ms before each beam crossing, providing a warmup time sufficient to stabilize the outputs before the arrival of a real signal. This power pulsing scheme reduces the power consumption and resulting heat generation of a tophat from nearly 500 W to approximately 60 W. Additionally, the power supplies, in racks on the top deck of the detector, only need to supply the average current, reducing supply and cable costs.

Tophat operations are directed locally by a controller board, which receives commands and timing signals from an external FASTBUS Timing and Control Module (TCM). Control signals are sent from the TCM on a set of three optical fibers – clock, command, data – using a standard SLD protocol. The signals are converted from optical to electrical form before arriving at the tophat. The tophat controller synchronizes all tophat operations — power pulsing, signal sampling, digitization and readout — to the TCM timing signals, and also controls various tophat operations, such as setting calibration voltages and channel calibration patterns.

The analog signal processing of the ionization charge collected on a calorimeter tower consists of amplification, shaping, sampling, analog storage, and digitization on a multiplexed ADC. Sensitive amplifier inputs are protected from high voltage discharges. A high precision internal calibration system is provided. The digitized signals are transmitted from the tophat to the FASTBUS system on top of the detector on optical fibers.

All of the analog functions are performed on preamplifier daughterboards. These daughterboards connect directly both to the cryostat feedthrough pins, to access the input signals from the calorimeter, and also to the tophat motherboard, for power, control, and output lines. Each barrel motherboard contains 15 daughterboards, each of which contains 48 channels of electronics, for a total of 720 channels per motherboard.

The preamplifier hybrids contain low noise, charge sensitive amplifiers followed by pulse shaping circuits and output drivers. Unipolar 4 μ s pulse shaping is used. The preamplifier hybrids also contain a calibration charge injection circuit for each preamp channel. The injected charge for each channel is equalized to an accuracy of 1/4 % by laser trimming a calibration capacitor.

A second custom hybrid circuit following the preamplifier provides analog signal storage and multiplexing. Shaped preamplifier signals are fed through high and low gain paths and stored as charges on capacitors. The signals are sampled twice, for a later peak – baseline subtraction.

Analog signals from the daughterboards are digitized to 12 bits on one analog-to-digital (A/D) conversion board per tophat. The data are multiplexed in a chain of parallel/serial shift registers, which are clocked out at a rate of 32 MHz by readout pulses from the controller board.

An optical driver converts the final serial bit stream to a series of light pulses, which is sent on a 50 meter long optical fiber to a FASTBUS rack on top of the detector. The transmission of optical data provides noise immunity in a compact cable. The entire LAC readout cable plant consists of one optical fiber per tophat.

3.2 Signal Range and Noise

The range of expected signals in the LAC is quite large, varying from a charge of 24 fC for a minimum ionizing particle traversing an EM1 tower to approximately 15 pC for a 46 GeV electromagnetic shower contained in a single EM tower. The dual gain amplification scheme in combination with 12-bit digitization gives an effective 15-bit dynamic range, allowing the full signal range to be covered with good resolution. At high gain one ADC count corresponds to an input charge of 5000 e^-, which is approximately equivalent to the rms noise on the smallest calorimeter channels.

The noise level of the LAC front-end electronics is dominated by the preamplifier FET input stage. The intrinsic noise of the preamplifier (expressed as equivalent charge at the input) is 2500 e^- in the absence of input capacitance. Digitization effects (ADC quantization) increase the actual noise of the full readout system to 4000 e^- (0.8 ADC count) at high gain. To achieve this noise performance on the detector, careful attention to grounding was necessary.

Noise in the LAC preamplifiers depends strongly on the input capacitance, increasing linearly with a slope of 2600 e^-/nF. The preamplifier pulse shaping time of 4 μs was chosen to optimize the tradeoff between intrinsic noise and the noise slope for capacitances of about 1 nF typical of EM2 calorimeter towers. In the EM1 section of the calorimeter, capacitances are smaller and the intrinsic noise term dominates. Noise in hadronic towers is dominated by the capacitive term, reaching 12000 e^- for the largest towers. Given the poorer intrinsic resolution of the calorimeter for hadron showers, this increased noise does not significantly degrade the hadronic resolution. For minimum ionizing particles, the signal to noise ratio is greater than 8:1 in all sections of the calorimeter. LAC tower capacitance ranges, noise, and signal sizes for minimum ionizing particles are collected in the following table.

Table 1. Tower Capacitance, Noise, MIP signal

Layer	Capacitance (pF)	Noise (e^-)	MIP dE/dX (e^-)
EM 1	350 – 600	4000	200000
EM 2	800 – 1300	5000 – 6000	500000
HAD 1	2500 – 3700	9000 – 12000	340000
HAD 2	2700 – 3800	9000 – 12000	340000

3.3 FASTBUS Electronics

The LAC FASTBUS plant uses just three basic types of modules: one Timing and Control Module (TCM), 32 Calorimetry Data Modules (CDMs), and one "Aleph Event Builder" (AEB). The TCM provides control and signals and timing strobes to the front-end electronics. The CDMs are responsible for receiving, correcting, and storing data from the front-end electronics. The AEB coordinates the operation of the CDMs and converts the data collected from the CDMs to the proper offline format for logging. The data from the entire LAC (40000 channels) is read out, digitized, and fully processed in FASTBUS every beam crossing.

The programmability of the AEB and CDMs results in a system capable of processing data in several ways. In normal data aquisition mode, the CDM selects the appropriate signal gain path, applies calibration constants to the baseline and signal buckets, and subtracts the calibrated baseline from the calibrated signal. The CDM also forms energy sums for use in the trigger decision. For triggered events, the CDM compacts the event data using layer dependent threshold cuts, and attaches a tower identification tag to each hit above threshold.

3.4 LAC Energy Trigger

In addition to normal tower readout, the FASTBUS system also provides the primary energy triggers for the SLD experiment. Local energy sums are computed in the FASTBUS CDMs every beam crossing, using the fully digitized and calibrated data from all towers. A relatively high trigger threshold (200-600 MeV) is applied to towers entering the trigger energy sum, to reject SLC beam-related backgrounds (particularly horizontal muons traversing many LAC towers parallel to the beamline). The local energy sums from all CDMs are combined in a trigger AEB, which uses a total energy requirement (or more complicated energy deposition requirements) to decide whether to trigger an event.

4. LAC Operational Performance

Test beams were unfortunately not available at SLAC during the period of LAC module construction, testing, and installation. The LAC was commissioned using cosmic rays in 1990 and 1991. A very successful 1992 data run was recently completed; during this run over 10000 Z^0 events were recorded in the SLD detector. Bhabha events recorded during this run provide a good test of the LAC performance for high energy electrons. Performance of the LAC for hadrons and jets can be studied using Z^0 hadronic decays. All of the performance studies using Z^0 data are preliminary; this very recent data is currently under intensive analysis.

4.1 Cosmic Ray Tests

The warm iron calorimeter (WIC) was used to provide unambiguous muon identification and to locate muon tracks in the LAC. The entire LAC was read out for each cosmic ray trigger. Calibration constants and a low threshold cut were applied online by the FASTBUS data acquisition system to each channel. The data analysis (and most of the event rate) was restricted to cosmic rays travelling nearly vertically downward. To select energetic muons passing through the entire detector, back-to-back hits were required in upper and lower WIC towers. Only calorimeter towers near the muon track in the lower half of the LAC were used in the analysis presented here. In each of the four longitudinal sections of the LAC, all hits in a window of 3x3 towers centered on the muon location were added together. A typical cosmic ray event is shown in figure 6.

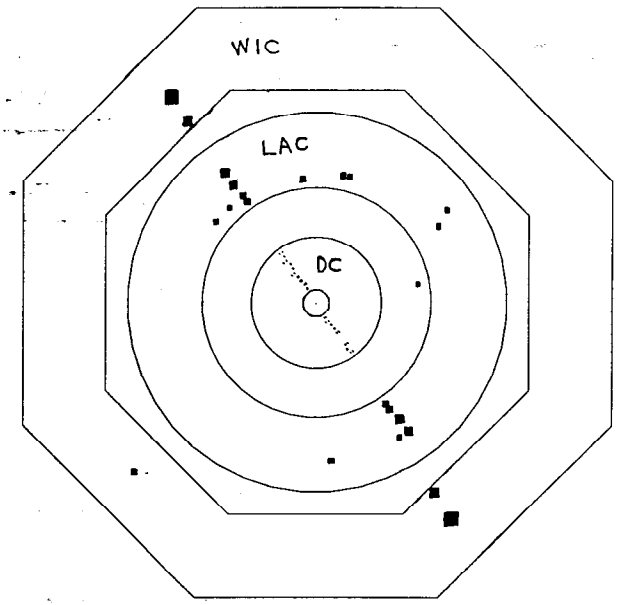

Figure 6. Cosmic ray muon in LAC and WIC.

Pulseheight distributions in the four LAC sections are shown in figure 7. Signals are well above noise in all layers. The pulseheight scale is proportional to the charge deposited in the liquid argon (argon/lead sampling is not included). Corrections for the high voltage blocking capacitors (~20%), argon charge collection efficiency (~5%), and the angle of incidence of the track (~5%) have been made. Arrows indicate the calculated mean energy loss for a minimum ionizing particle traversing the argon in each section. The data agree well with expectations.

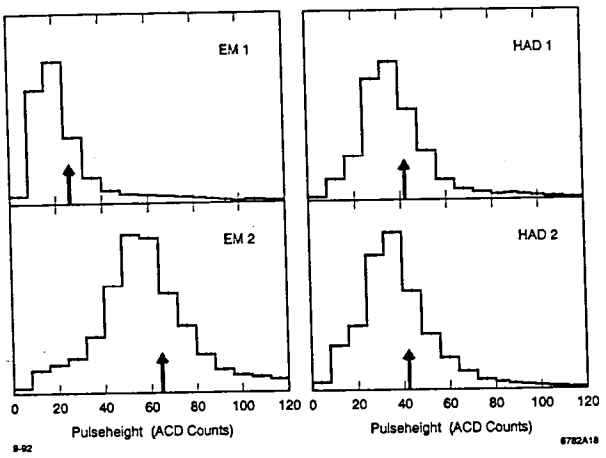

Figure 7. Cosmic ray muon pulseheight distributions in the LAC.

The response of the LAC as a function of high voltage has also been studied using cosmic rays. The LAC is normally operated at 2000 volts; test data were taken with voltages from 3000 volts down to 250 volts. Cosmic ray signals in the LAC are shown in figure 8 as a function of voltage. The signal decreases with decreasing voltage because the electron drift path length decreases, allowing more charge to be captured by electronegative impurities, and because recombination of the liquid argon ions and electrons increases as the drift velocity decreases. The curve shows the predicted response of the LAC with 0.7 ppm of oxygen in the liquid argon. This level of contamination is consistent with independent measurements of the argon taken before filling the detector.

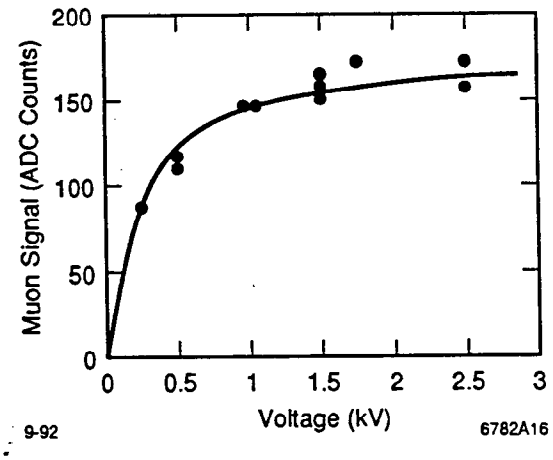

Figure 8. High voltage plateau using cosmic ray muons.

4.2 Bhabha electrons

Bhabha events provide an ideal calibration point for the electromagnetic LAC. A typical event, with the Bhabha electrons detected in the LAC endcaps, is shown in figure 9. The events are very clean at this energy scale. Note that the full granularity of the LAC is not shown – each bin in the plot actually includes a 2x4 array of towers, and the EM1 and EM2 longitudinal layers have been summed.

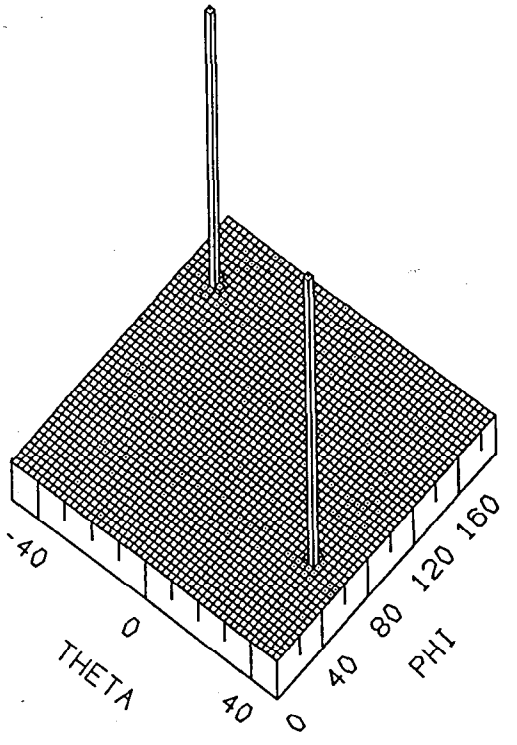

Figure 9. Bhabha event in the LAC (barrel and endcaps unfolded).

The pulseheight distribution for several hundred Bhabha electrons in the barrel LAC is shown in figure 10. Events were selected by requiring two back-to-back electrons in the central region $|\cos(\theta)| < 0.4$. The overall LAC energy scale will ultimately be set using this class of events. The energy resolution presently achieved is $\sigma/\mathrm{E} = 2.3\%$, corresponding to a scaling term of $15\%/\sqrt{(E)}$.

The resolution in the endcap LAC appears considerably worse, possibly due to increased material in front of the detector. The endcap response and resolution is still under investigation.

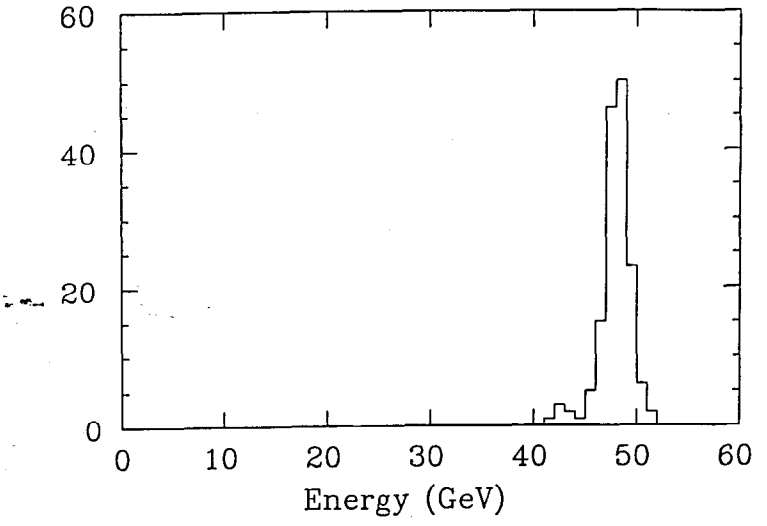

Figure 10. Bhabha electron resolution in barrel LAC.

The angular resolution of the LAC has also been studied using Bhabha electrons, tracked by the central drift chamber and extrapolated to the calorimeter. Using a simple shower centroid position in the LAC, an angular resolution of 5-10 mrad is observed; this is considerably smaller than the typical tower size of about 33 mrad.

4.3 Hadrons and Jets

We have just begun to study the LAC performance for hadrons and jets. Isolated tracks provide a reasonably clean source of pions with momenta in the few GeV range. Very preliminary studies indicate an energy resolution of roughly $60\%/\sqrt{(E)}$ for these particles.

Jets of hadrons are of course copiously produced in Z^0 decays, but our analysis has not progressed far enough to present any resolution figures. For jets, it is important to correctly include energy leaking out of the LAC into the WIC, and this problem is still being worked on.

A typical two-jet event in the LAC is shown in figure 11. The granularity of the bins is again 2x4 towers, with all EM and HAD layers summed.

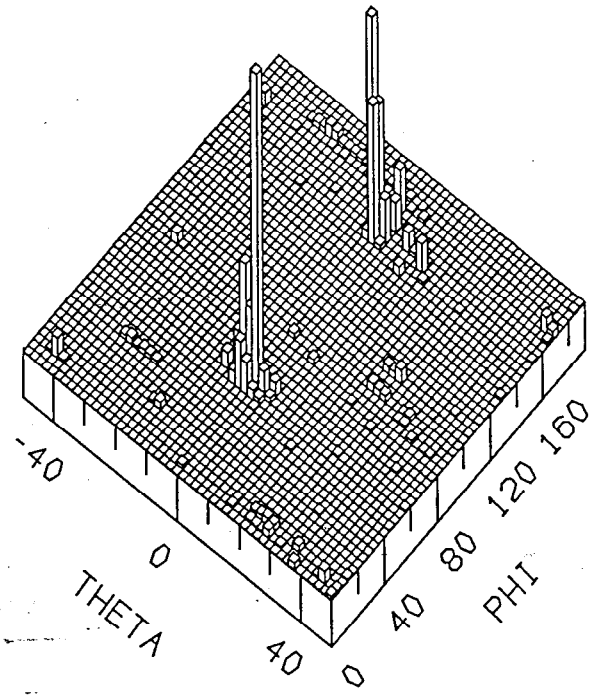

Figure 11. Hadronic Z decay to two jets in LAC.

5. Acknowledgments

Many members of the SLD collaboration have contributed to the successful construction and operation of the LAC. Only a few can be mentioned here. Calorimeter modules were built by physicists at Caltech (D. Hitlin, W. Wisniewski, G. Eigen, M. Kelsey), the University of British Columbia (R. Sobie), TRIUMF (C. Oram), the University of Victoria (A. Honma, M. Turcotte), the University of Washington (P. Mockett, E. Vella, H. Kim), and Columbia University (P. Rowson, T. Bolton, S. Smith, A. Bazarko). Engineering, cryogenics, and electronics were primarily the responsibility of SLAC engineers and physicists (M. Breidenbach, R. Schindler, I. Abt, R. Dubois, J. Labs, T. Junk, H. Neal, A. Waite). Analysis presented in this paper was the result of efforts by E. Vella, P. Rowson, A. Bazarko, R. Dubois, J. Yamartino, S. Gonzalez.

6. References

[1] D. Axen *et. al.*, "The Lead - Liquid Argon Sampling Calorimeter of the SLD Detector," SLAC-PUB-5354 (1992), to be published in *Nucl. Inst. Meth. A.*